European Heart Journal Open (2023) **3**, 1–12
https://doi.org/10.1093/ehjopen/oead088

ORIGINAL ARTICLE
Coronary artery disease

Artificial intelligence–based opportunistic detection of coronary artery stenosis on aortic computed tomography angiography in emergency department patients with acute chest pain

Carl G. Glessgen [1,*], Marianthi Boulougouri[1], Jean-Paul Vallée [1], Stéphane Noble[2], Alexandra Platon[1], Pierre-Alexandre Poletti[1], Jean-François Paul [3], and Jean-François Deux[1]

[1]Department of Radiology, Geneva University Hospitals, Rue Gabrielle-Perret-Gentil 4, Geneva 1205, Switzerland; [2]Department of Cardiology, Geneva University Hospitals, Rue Gabrielle-Perret-Gentil 4, Geneva 1205, Switzerland; and [3]Department of Radiology, Cardiac Imaging, Institut Mutualiste Montsouris, Paris 75014, France

Received 12 July 2023; revised 8 August 2023; accepted 6 September 2023; online publish-ahead-of-print 7 September 2023

Aims

To evaluate a deep-learning model (DLM) for detecting coronary stenoses in emergency room patients with acute chest pain (ACP) explored with electrocardiogram-gated aortic computed tomography angiography (CTA) to rule out aortic dissection.

Methods and results

This retrospective study included 217 emergency room patients (41% female, mean age 67.2 years) presenting with ACP and evaluated by aortic CTA at our institution. Computed tomography angiography was assessed by two readers, who rated the coronary arteries as 1 (no stenosis), 2 (<50% stenosis), or 3 (≥50% stenosis). Computed tomography angiography was categorized as high quality (HQ), if all three main coronary arteries were analysable and low quality (LQ) otherwise. Curvilinear coronary images were rated by a DLM using the same system. Per-patient and per-vessel analyses were conducted. One hundred and twenty-one patients had HQ and 96 LQ CTA. Sensitivity, specificity, positive predictive value, negative predictive value (NPV), and accuracy of the DLM in patients with high-quality image for detecting ≥50% stenoses were 100, 62, 59, 100, and 75% at the patient level and 98, 79, 57, 99, and 84% at the vessel level, respectively. Sensitivity was lower (79%) for detecting ≥50% stenoses at the vessel level in patients with low-quality image. Diagnostic accuracy was 84% in both groups. All 12 patients with acute coronary syndrome (ACS) and stenoses by invasive coronary angiography (ICA) were rated 3 by the DLM.

Conclusion

A DLM demonstrated high NPV for significant coronary artery stenosis in patients with ACP. All patients with ACS and stenoses by ICA were identified by the DLM.

* Corresponding author. Tel: +41 79 55 36 227, Email: carl.glessgen@hcuge.ch
© The Author(s) 2023. Published by Oxford University Press on behalf of the European Society of Cardiology.
This is an Open Access article distributed under the terms of the Creative Commons Attribution-NonCommercial License (https://creativecommons.org/licenses/by-nc/4.0/), which permits non-commercial re-use, distribution, and reproduction in any medium, provided the original work is properly cited. For commercial re-use, please contact journals.permissions@oup.com

Graphical Abstract

Key question

Assessing the precision of an AI model in detecting coronary stenoses from routinely performed aortic CTA in emergency patients with suspected aortic dissection.

Key findings

Model achieves 100% sensitivity for significant stenoses on high-quality CTA, 79% on low-quality scans.
All patients with ACS and stenoses by ICA were identified.

Take-home message

AI model proves effective as supplemental diagnostic tool for opportunistic coronary stenosis detection in patients with suspected aortic dissection.

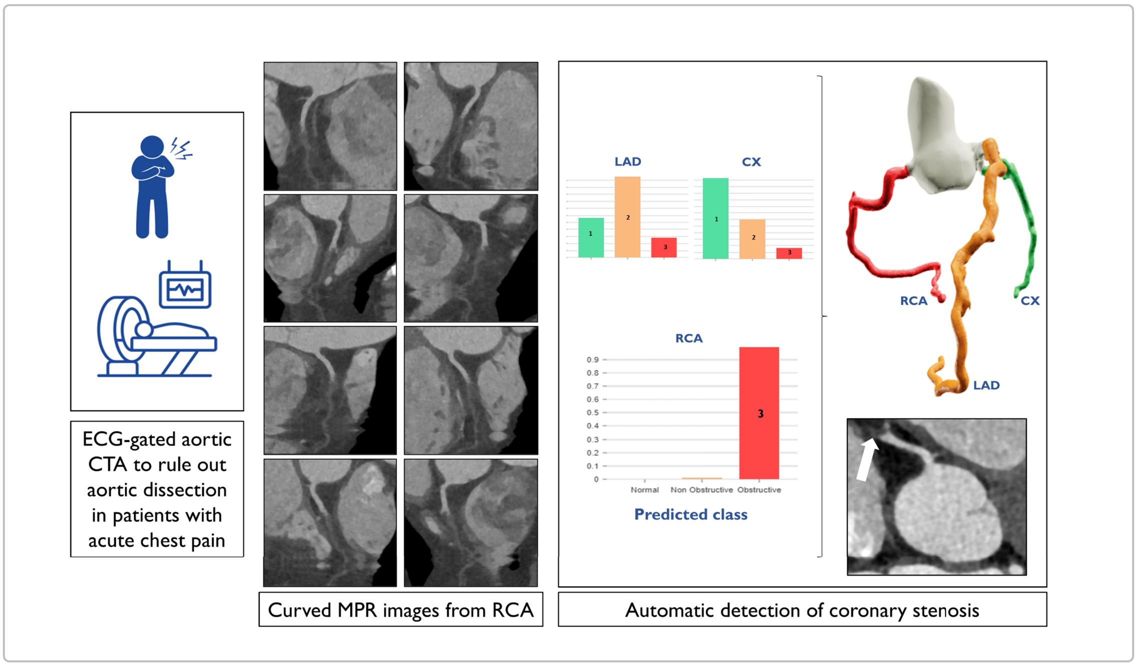

Study highlights and presentation of the study workflow. Showcase of a proximal RCA occlusion opportunisticall identified by the AI model in a 54 year-old male patient with acute chest pain. ACS, acute coronary syndrome; AI, artificial intelligence; CTA, computed tomography angiography; CX, circumflex artery; ECG, electrocardiogram; ICA, invasive coronary angiography; LAD, left anterior descending artery; MPR, multiplanar reconstruction; RCA, right coronary artery.

Keywords Computed tomography angiography • Cardiac-gated imaging techniques • Chest pain • Deep learning • Coronary artery disease

Introduction

Acute chest pain (ACP) is a common emergency that often prompts hospital admission.[1,2] Life-threatening causes of ACP such as acute coronary syndrome (ACS), acute aortic syndrome (AAS), and pulmonary embolism must be identified promptly.[3–5] However, the symptoms vary widely and overlap with those of benign conditions such as musculoskeletal pain, gastroesophageal reflux, and pleuritis. When the history, physical examination, biomarkers, and electrocardiogram (ECG) fail to convincingly establish the diagnosis, imaging studies are valuable. Among them, ECG-gated aortic computed tomography angiography (CTA) plays a pivotal role to rule out aortic dissection and is routinely performed.[6–8] Electrocardiogram-gating attenuates aortic pulsation artefacts and visualizes the aortic root clearly, thereby aiding in the diagnosis of AAS. Even though beta-blockers and vasodilator preparation are generally not used in this emergency setting, coronary arteries may be visualized on computed tomography (CT) images and coronary stenoses identified, potentially leading to alternate diagnoses.[9,10] However, physicians with dedicated experience in cardiac imaging are not always available during shifts. Moreover, emergency room radiologists often face overwhelming workloads, and analysing coronary CTA images is a time-consuming task.

Computer-assisted diagnosis solutions have been proposed previously to support radiologists in identifying acute pathologies on CT images, such as pulmonary embolism or intra-cranial haemorrhage.[11,12] Likewise, using deep-learning models (DLMs) for coronary CTA images could be promising in helping to avoid the oversight of coronary stenoses. In stable patients, seen in non-emergent settings and explored with dedicated cardiac CT, several DLMs have been reported to perform at least as well as specialized physicians for detecting coronary stenoses.[13–20] Yet, no large-scale study has assessed the performance of DLMs to identify coronary stenoses in patients seen in the emergency room and explored with an ECG-gated aortic CTA to rule out aortic dissection.

The objective of this retrospective observational work was therefore to evaluate the performance of a DLM for detecting coronary artery stenosis in patients who presented to the emergency room for ACP and underwent routine ECG-gated aortic CTA to rule out aortic dissection. Our working hypothesis was that a DLM would perform well in detecting coronary artery disease, thus potentially improving diagnosis confidence for human analysis.

Methods

This single-centre, retrospective, observational study was approved by the local ethics committee (ID 2022-01814). In compliance with Swiss law on retrospective analyses of de-identified health data, the committee waived the requirement for informed consent.

Study population

Figure 1 is the patient flow chart. We searched the institutional database and reviewed the records of consecutive patients who underwent CTA to assess ACP at the emergency room of our institution between January 2020 and May 2022. During the image analysis process, we excluded patients with CTA evidence of coronary stenting or bypass surgery, failed arterial bolus-chasing [aortic density values beneath 200 Hounsfield unit (HU)], or destructive respiratory artefacts precluding cardiac volume analysis.

Data collection

For each patient, we used standardized forms to collect age, sex, body mass index, mean heart rate during CTA, blood troponin and brain natriuretic peptide (BNP) levels, and glomerular filtration rate (GFR) estimated using the CKD-EPI creatinine equation. We recorded the presence of diabetes, hypertension, and dyslipidaemia, as well as the discharge diagnosis established on the basis of all available data. When invasive coronary angiography (ICA) was performed after CTA, the report was collected.

Image acquisition

The same, third-generation, dual-source CT scanner (SOMATOM Force; Siemens Healthineers, Erlangen, Germany) and imaging protocol used for suspected aortic dissection were used in all included patients. No beta-blockers or sublingual nitrates were administered.

A high-pitch cardiac scan with prospective ECG gating was acquired before contrast administration to identify intramural haematoma. A prospective ECG-gated high-pitch helical scan encompassing the whole aorta was then acquired in breath-hold at 60% of the R–R interval. Scanner parameters were as follows: 0.6 mm collimation, 3.2 helicoidal pitch, 70–120 kV tube voltage, and 162–499 mAs tube current–time product. Iodinated contrast (Acupaque 350; GE Healthcare AG, Glattbrugg, Switzerland) was injected intravenously at a fixed volume of 80 mL and a flow rate of 4–5 mL/s, using a power injector, followed by 20 mL of saline chaser. The acquisitions were triggered through bolus tracking using a region of interest in the ascending aorta and a threshold of 100 HU with a fixed 10 s delay. In addition, the scanner automatically performed smaller field of view (FOV) reconstructions dedicated to the ascending aorta and aortic root visualization with the following parameters: 512-by-512 matrix reconstruction, Bv36d convolution kernel, 19×19 cm FOV, and 0.6 mm section thickness.

Image analysis

The ROIs were traced manually by one author (M.B.) on the enhanced CT images of the ascending aorta to record mean attenuation (HUs). Calcium scores were extracted automatically from the unenhanced CT images on a dedicated platform (SyngoVia, version VB20A; Siemens Healthineers).

Two radiologists (C.G.G. and J.-F.D.) with respectively 2 and 20 years of experience in cardiac imaging (equivalent to Society of Cardiovascular Computed Tomography Levels 2 and 3, respectively) interpreted the CT data sets by consensus. Both readers had only basic experience with the DLM under evaluation. The reading was performed using the smaller FOV reconstructions of the aortic root that were loaded on the same platform. Readers reviewed the axially enhanced coronary images, multiplanar reconstruction (MPR) images, and curvilinear MPR images of the left anterior descending artery, circumflex artery (CX), and right coronary artery using the dedicated platform.

Patients were classified as having low-quality (LQ) CTA images if at least one artery was not analysable and as having high-quality (HQ) CTA images if all three arteries were analysable. Minimal artefacts not interfering with the analysis did not change the HQ status. *Figure 2* shows examples of CTA images from patients in the HQ and LQ groups.

Each analysable coronary artery was graded on a three-point scale using a simplified CAD-RADS (Coronary Artery Disease-Reporting and Data System) classification,[21] as follows: (i) no stenosis; (ii) 1–49% stenosis; and (iii) 50% stenosis or more. In the HQ group, a global score (1, 2, or 3) was attributed to each patient on the basis of the highest class among the three arteries.

To assess inter-rater agreement, we used a random sample of 20% of the overall population. At least 3 months after the first reading, the images for these patients were assessed again by the same two readers by consensus, using the same scoring system as for the first reading.

Deep-learning model

The previously described CorEx model (version 1.0; Spimed-AI, Bourg-la-Reine, France) was used.[20] Briefly, this model was trained using the Inception-v3 convolutional neural network developed by Google[22] over a cohort of 400 coronary CTA cases. Training weights were initialized using a random normal function, and the first layers of the model were expanded to improve low-level feature detection. The softmax function was employed for output activation. As input, the model accepts curved MPR images comprising radial reconstructions 40° apart over the full vessel circumference (9 images per vessel, i.e. 27 images per patient). The model applies the simplified CAD-RADS classification described above and assigns each class a probability for the input vessel.

For the present study, the curved MPR images were created automatically from enhanced CT images as described above and exported, without prior modification, by one of the readers (C.G.G.) to a local server harbouring the DLM. The class for each vessel (1, 2, or 3) predicted by the DLM to be most likely and the global class for each patient (1, 2, or 3) were recorded. Both processing of MPR images and collection of stenosis classes were performed later and at a distance from the human grading.

Statistical analysis

Quantitative variables had a non-normal distribution, as assessed using the Shapiro–Wilk test, were described as median [interquartile range (IQR)], and then compared between the HQ and the LQ groups by applying the non-parametric Mann–Whitney U test. Categorical variables were described as number (%) and compared between the HQ and the LQ groups using Pearson's χ^2 test with Yates' continuity correction. Categorical variables with fewer than five values were not compared. Deep-learning model output was compared with the results of the consensus evaluation by the two readers (ground truth) taken as the reference standard for each vessel and each patient. Sensitivity, specificity, positive predictive value (PPV), negative predictive value (NPV), and accuracy were calculated for each DLM analysis. Inter-reader agreement on the random subsample was assessed by computing Cohen's kappa coefficient. P-values of 0.05 or less were considered significant. Statistical analysis was conducted using RStudio (2022.07.0 + 548) for R (R Foundation for Statistical Computing, Vienna, Austria) and Python (v. 3.9.12, Python Software Foundation, Wilmington, DE, USA).

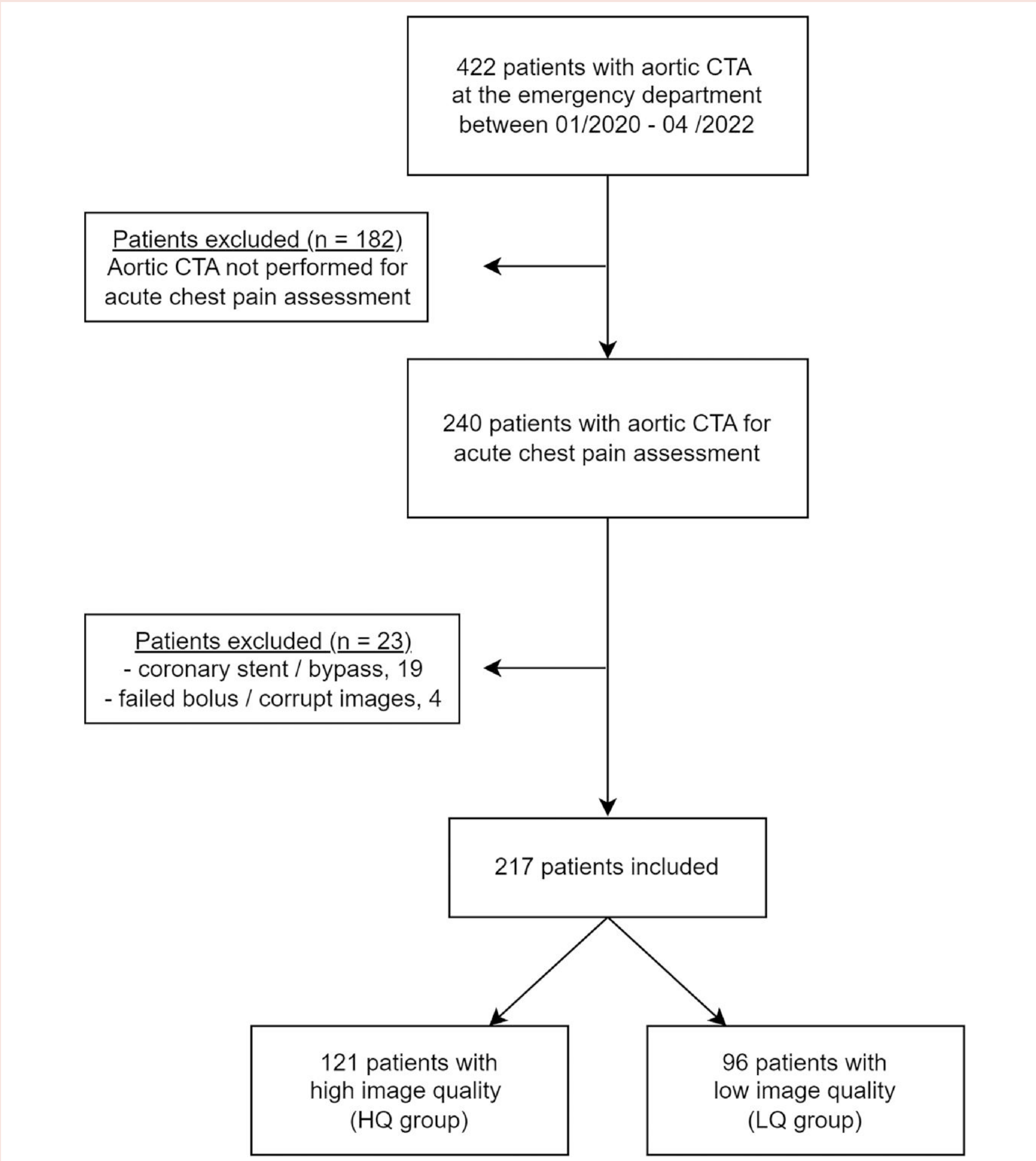

Figure 1 Patient flow chart. Emergency room patients sent to the radiology department for assessment of acute chest pain were included. Patients with prior coronary interventions or corrupt image quality were excluded.

Results

We included 217 patients, whose main characteristics are reported in *Table 1*. Among them, 121 were in the HQ group and 96 in the LQ group. The heart rate was significantly higher in the LQ group. None of the other parameters differed between groups.

Performance of the deep-learning model in the high-quality group

Of the 121 patients, 43 (36%) were Class 3 (stenosis ≥50%) by human reading. All 43 were identified by the DLM. Of the 78 remaining patients, 40 (51%) were Class 1 and 38 (49%) Class 2 by human reading,

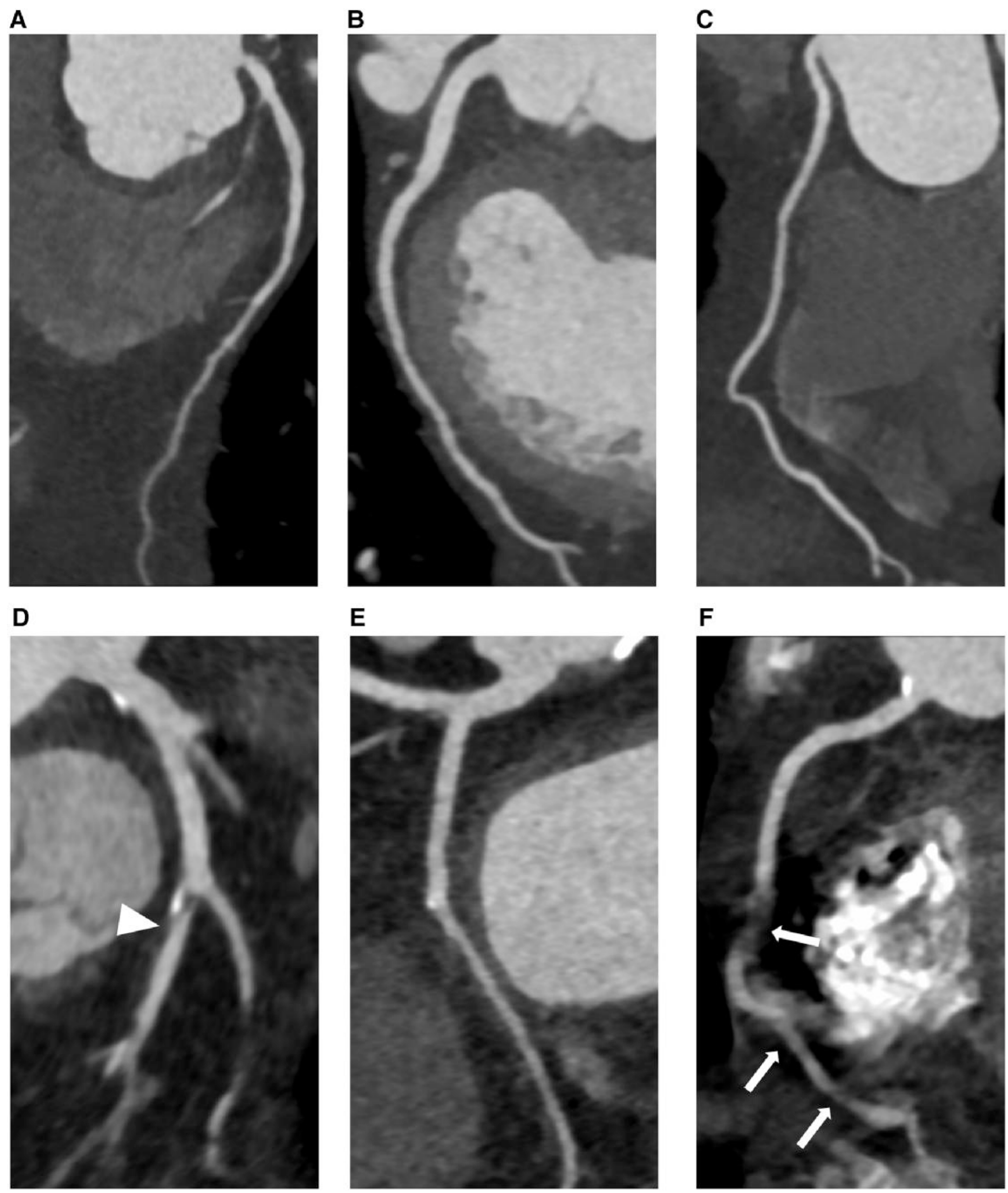

Figure 2 Examples of curvilinear reconstructions in groups with high- and low-quality images. Reconstructions of the left anterior descending artery (*A* and *D*), circumflex artery (*B* and *E*), and right coronary artery (*C* and *F*) in a patient with high-quality images (top) and another with low-quality images (bottom). In patients with high-quality images, the readers and deep-learning model assigned the left anterior descending artery, circumflex artery, and right coronary artery to Classes 2, 2, and 1, respectively. In a patient with low-quality images, the readers considered that the left anterior descending artery and circumflex artery were analysable but that the right coronary artery was not, due to extensive motion artefacts (arrows, *F*). The readers and deep-learning model assigned the left anterior descending artery to Class 3 (significant stenosis in the middle segment, arrow, *D*) and the circumflex artery to Class 2.

whereas 7 (9%) were Class 1, 41 (52%) Class 2, and 30 (38%) Class 3 by DLM reading. Consequently, the sensitivity, specificity, PPV, NPV, and accuracy of the DLM in detecting patients rated Class 3 (≥50% stenosis) were 100, 62, 59, 100, and 75%, respectively (*Table 2*). Per-class comparisons between DLM and expert consensus are reported in *Figure 3*.

Of the 363 coronary arteries, 80 (22%) were rated Class 3 (≥50% stenosis) by human reading. The DLM accurately identified 78 (97%) of these vessels and categorized the remaining two vessels as Class 2. Of the 283 (78%) vessels classified as Class 1 ($n = 168$) or Class 2 ($n = 115$) by human reading, 225 (79%) were also Class 1 or 2 according to the DLM and 58 (21%) were Class 3. Consequently, the sensitivity,

Table 1 Main features of the patients at emergency department presentation

Variables[a]	Overall ($n = 217$)	HQ group ($n = 121$)	LQ group ($n = 96$)	*P*-value
Females, *n* (%)	89 (41)	52 (43)	37 (38)	0.60
Age, years	68 (57–80)	69 (58–82)	67 (57–77)	0.43
Body mass index, kg/m^2	26.2 (22.9–29.0)	26.6 (23.1–29.2)	25.6 (21.6–28.0)	0.11
Cardiovascular risk factors, *n* (%)				
Diabetes	39 (18.0)	22 (18.2)	17 (17.8)	0.99
Hypertension	154 (71.0)	88 (72.7)	66 (68.8)	0.41
Dyslipidaemia	64 (29.5)	33 (27.3)	31 (32.3)	0.51
Laboratory parameters[b]				
Troponin, ng/L	20 (8–57)	21 (8–54)	18 (7–64)	0.92
BNP, ng/L	551 (137–1855)	796 (263–2377)	324 (75–1215)	0.07
Glomerular filtration rate, mL/min/1.73 m^2	81 (58–98)	82 (60–99)	78 (50–95)	0.16
Heart rate, b.p.m.	72 (61–86)	65 (58–83)	78 (68–88)	<0.01
Coronary artery calcium Agatston score	86 (0–465)	65 (0–496)	95 (2–448)	0.51
Blood pool attenuation, HU	426 (330–552)	437 (343–564)	437–145	0.10
Discharge diagnosis, *n* (%)				
Gastrointestinal condition	34 (15.7)	15 (12.4)	19 (19.8)	0.19
Acute aortic syndrome	20 (9.2)	8 (6.6)	12 (12.5)	0.21
Acute aortic disorder	13 (6.0)	9 (7.4)	4 (4.2)	0.47
Heart failure	20 (9.2)	11 (9.1)	9 (9.4)	0.99
ACS [(N)STEMI, unstable angina]	17 (7.8)	9 (7.4)	8 (8.3)	0.75
Chest wall pain	17 (7.8)	10 (8.3)	7 (7.3)	0.99
Hypertensive crisis	12 (5.5)	10 (8.3)	2 (2.1)	0.09
Pneumonia	9 (4.2)	5 (4.1)	4 (4.2)	NA
Pericarditis	7 (3.2)	5 (4.1)	2 (2.1)	NA
Pulmonary embolism	5 (2.3)	3 (2.5)	2 (2.1)	NA
Panic disorder	3 (1.4)	2 (1.7)	1 (1.0)	NA
Other[c]	60 (27.6)	30 (24.8)	30 (31.3)	0.37

[a]Quantitative variables are reported as median (IQR).
[b]Based on available data, carried out at admission to the emergency department.
[c]No identified cause or condition that does not typically manifest as chest pain (e.g. electrolyte disturbances).

Table 2 Performance of the deep-learning model at patient and vessel levels in the two image-quality groups

Image-quality group	Level	Sensitivity (%)	Specificity (%)	PPV (%)	NPV (%)	Accuracy (%)
High quality	Patient	100	62	59	100	75
	Vessel	98	79	57	99	84
Low quality	Patient	—	—	—	—	—
	Vessel	79	86	71	90	84

specificity, PPV, NPV, and accuracy of the DLM in detecting vessels with ≥50% stenoses (i.e. Class 3) were 98, 79, 57, 99, and 84%, respectively (*Table 2*). Per-class comparisons between DLM and expert consensus are reported in *Figure 3*. Examples of mismatch between DLM and human readings are reported in *Figure 4*.

Performance of the deep-learning model in the low-quality group

No patient class was assigned by human readers to this group of patients because of partially non-analysable coronary arteries. Of the 96 patients, 2 (2%) were assigned by the DLM to Class 1, 19 (20%) to Class 2, and 75 (78%) to Class 3.

Of the 288 vessels, 134 vessels (46%) were considered non-analysable by human reading. Among them, 11 (8%) were assigned by the DLM to Class 1, 39 (29%) to Class 2, and 84 (63%) to Class 3.

Of the 154 analysable vessels, 47 (31%) were assigned to Class 3 (≥50% stenosis) by human reading; among them, 37 (79%) were DLM Class 3 and 10 (21%) were DLM Class 2. Of the 107 (69%) vessels assigned to Class 1 or 2 by human reading, 92 (86%) were DLM Class 1 or 2 and 15 (14%) were DLM Class 3. Consequently, the sensitivity,

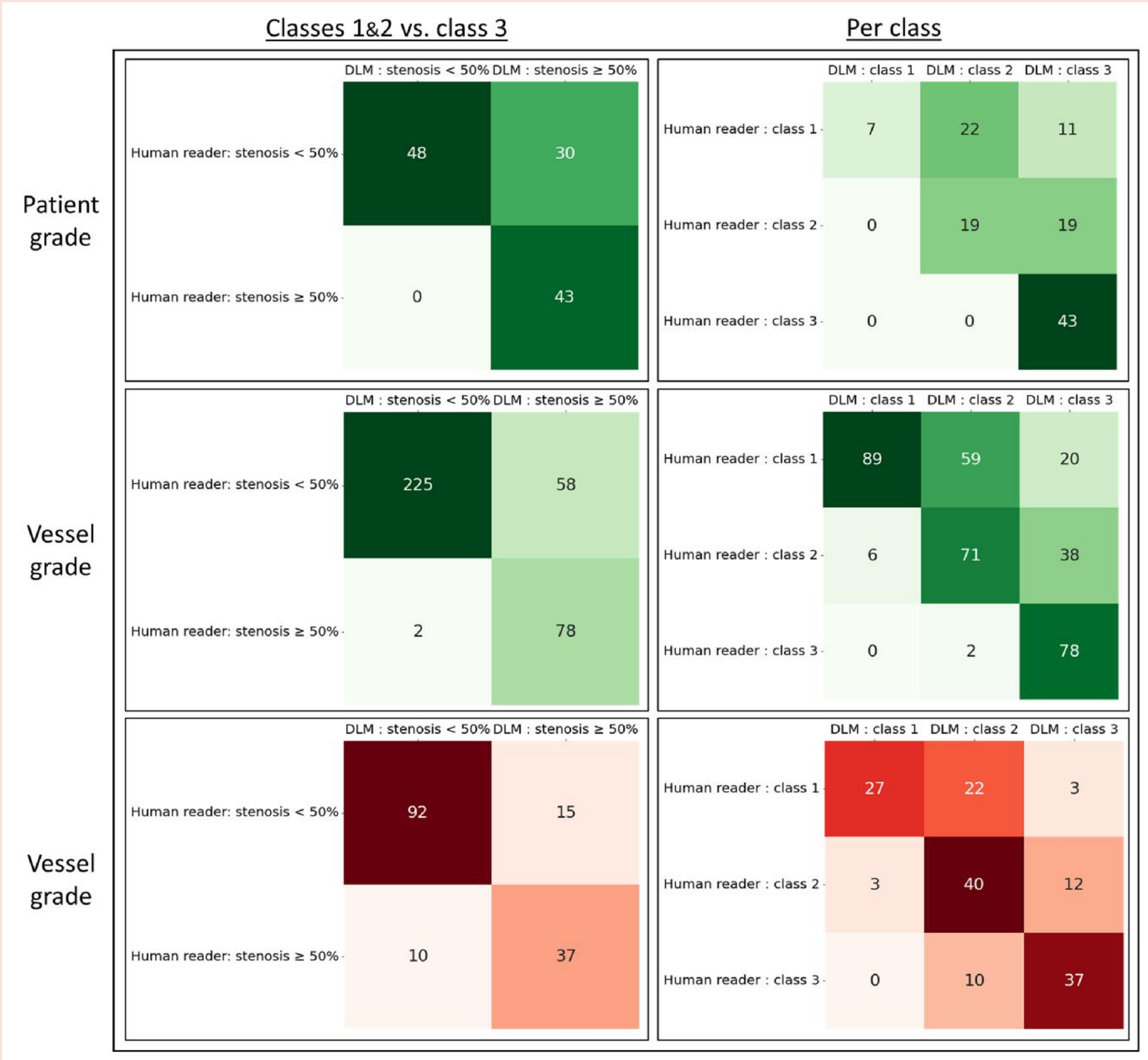

Figure 3 Distribution of patients and vessels across stenosis grades in both high-quality (first two lines) and low-quality (bottom line) groups. Patients in the low-quality group (bottom line) had at least one vessel deemed uninterpretable so that patient-level comparisons were not feasible. Consequently, low-quality cases were assessed only at the vessel level. The results are presented as confusion matrices of classes assigned by the readers and deep-learning model. In the first column, Classes 1 and 2 are collapsed into a single group with non-significant (<50%) or no stenosis. The second column reports the confusion matrix for each individual stenosis class.

specificity, PPV, NPV, and accuracy of the DLM in detecting ≥50% stenoses (i.e. Class 3) in analysable vessels were 79, 86, 71, 90, and 84%, respectively (*Table 2*). Per-class comparisons between DLM and expert consensus are reported in *Figure 3*.

Performance in patients diagnosed with acute coronary syndrome

A final discharge diagnosis of ACS was recorded for 17 (7.8%) patients, including 16 with myocardial infarction (non-ST-elevation myocardial infarction, NSTEMI: 10/16, ST-elevation myocardial infarction, STEMI: 6/16) and 1 with unstable angina. No patient had an ACS due to or associated with AAS. Three patients did not qualify for ICA: one patient had malignant embolism, another had no coronary stenosis by CTA and low troponin levels, and the third haemodynamic instability followed by death in the emergency room. Of the remaining 14 patients, 12 had ≥50% stenosis or occlusion. All 12 were assigned to Class 3 by the DLM (5 in the HQ group and 7 in the LQ group). At the vessel level, sensitivity, specificity, PPV, NPV, and accuracy of the DLM for detecting Class 3 stenoses were 93, 85, 90, 87, and 89%, respectively (*Graphical Abstract*); in the HQ group, corresponding values were 100,

Figure 4 Examples of a mismatch between human analysis and deep-learning model at vessel level. (*A* and *B*) Stenosis of the distal part of the right coronary artery caused by a soft plaque (arrow heads), classified as Class 3 by the human reader and Class 2 by the deep-learning model. (*C* and *D*) Left anterior descending artery without significant stenosis but sparsely calcified plaques (arrows), rated Class 2 by the human reader and Class 3 by the deep-learning model.

89, 86, 100, and 93%, respectively, and in the LQ group, they were 88, 75, 88, 75, and 83%, respectively. *Table 3* provides further details. Illustrated case-based examples are presented in *Figures 5* and *6*.

Reproducibility

Inter-reader agreement between first and second readings for detecting Class 3 (≥50%) stenosis was high at both the patient ($\kappa = 0.79$) and vessel ($\kappa = 0.84$) levels. Inter-reader agreement for specific stenosis classes was slightly lower (patient level, $\kappa = 0.72$; and vessel level, $\kappa = 0.65$).

Discussion

This retrospective single-centre study evaluated the performance of a recently introduced DLM for coronary stenosis identification in a cohort of emergency room patients with ACP who underwent diagnostic CTA. To our knowledge, this is the first study reporting the use of a DLM for coronary stenosis detection on CTA images acquired in an acute emergency room setting, with CTA protocols that were not optimized for evaluating the coronary artery. The main results were as follows: (i) sensitivity and NPV were high in patients with HQ images; (ii) all patients with subsequently identified ACS and stenoses by ICA in both the HQ

Table 3 Deep-learning model performance in patients discharged with a diagnosis of acute coronary syndrome who underwent invasive coronary angiography

Age (years)	Sex	Coronary calcium score	Image-quality group	Patient DLM class	LAD DLM class	CX DLM class	RCA DLM class	SS[a] by ICA	Location of lesions by ICA
90	F	121	HQ	3	3	1	2	Y	Acute LAD occlusion
74	F	1005		3	3	2	3	Y	Triple-vessel disease
39	M	0		2	2	1	2	N	LAD plaque rupture without SS
54	M	0		3	1	1	3	Y	Acute RCA occlusion
74	M	418		3	3	3	2	Y	Acute CX occlusion
51	M	19		3	2	1	3	Y	Acute diagonal branch occlusion
55	M	258	LQ	3	3	1	3	Y	Triple-vessel disease
67	M	713		3	3	2	3	Y	Acute LAD occlusion
76	M	923		3	2	3	3	Y	Triple-vessel disease
71	F	1356		3	3	3	2	Y	Acute RCA occlusion (distal part)
69	F	0		3	2	1	3	N	LAD plaque rupture without SS
85	M	1978		3	3	3	3	Y	Triple-vessel disease
76	M	617		3	3	2	3	Y	SS of LAD, chronic RCA occlusion
63	M	54		3	3	2	2	Y	Acute marginal branch occlusion, SS of LAD

[a]Significant stenosis (SS) defined as ≥50%.

and the LQ groups were assigned to Class 3 (≥50% stenosis) by the DLM.

Our DLM was recently introduced by Paul *et al.*,[20] who reported slightly lower sensitivity (93%) but higher specificity (97%) compared with our results. In this initial study, the patients had chronic chest pain or cardiovascular risk factors and underwent optimized coronary CTA, potentially explaining the higher specificity. In addition, the DLM used was trained over CTA images from scanners from different vendors and using partly different CT parameters than the ones used in this study. This could have influenced its performance over our data set. From a more general point of view, the performance characteristics of the DLM in both image-quality groups in the current study compare favourably with those reported for other DLMs applied to dedicated coronary CTA performed in non-emergent settings, whose sensitivity and specificity for detecting ≥50% stenosis ranged from 58 to 95%.[14,15,17–19,21,22] Of note, in both image-quality groups, all patients with ≥50% stenoses by radiologist-read CTA who received a diagnosis of ACS and had stenoses by ICA also had ≥50% stenoses detected by the DLM, underlining the potential of artificial intelligence (AI) for identifying such patients.

The diagnostic accuracy of the DLM at the vessel level was the same (84%) in the HQ and LQ groups. The lower sensitivity in the LQ group (79%), which had a significantly higher median heart rate vs. the HQ group (78 vs. 65 b.p.m., $P < 0.01$), is probably related to our use of a CTA protocol designed for vascular imaging but not optimized for imaging the coronary artery, with a high-pitch acquisition at 60% of the R–R interval.[23] Sequential or systole-centred acquisition in patients with tachycardia would probably have decreased the prevalence of LQ imaging. In the future, DLM training with images that are of suboptimal quality but suitable for interpretation might improve performance in evaluating LQ cases. Another avenue towards improvement might be the addition of a DLM confidence score based on image quality to alert emergency physicians to the risk of potentially inaccurate classification.

In this study, we report a rate of AASs (9%), which remains in the range of previous studies.[6,24] Coronary stenoses were relatively common (36% of ≥50% stenosis in the HQ group), but consistent with previous studies that used dedicated cardiac CT in emergency room patients: 31% in the study by Hoffmann *et al.*[25] and 32% in the study by Dedic *et al.*[26] The 8% rate of ACS that we report here is in line with studies that used dedicated cardiac CT in patients with ACP, ranging from 4 to 17%.[25–27] This comparable ACS rate despite the different population selection may be due to differences in clinical management between institutions.

Coronary arteries were often analysable in our study despite a non-dedicated cardiac imaging. While most stenoses detected were not responsible for ACP in our study, a certain number was underlining the interest of an opportunistic analysis of coronary arteries. Having an AI in this context could improve the diagnostic confidence of the human reader in the analysis of coronary vessels. As a result, we report an opportunistic analysis of coronary arteries on an aortic CTA. Our study, however, does not support a systematic evaluation of the coronary vessels, aorta, and pulmonary arteries, otherwise known as the triple-rule-out technique. This

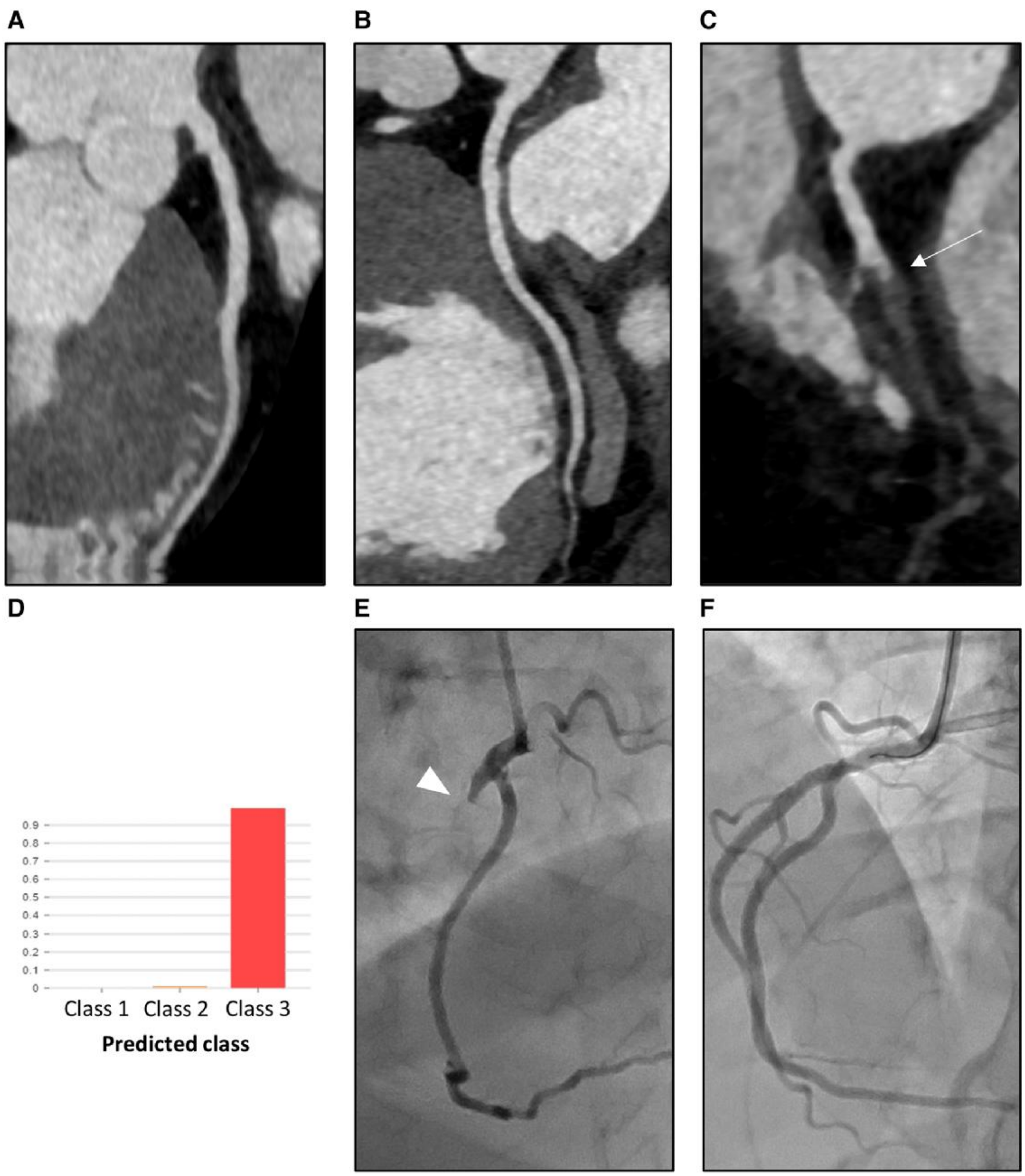

Figure 5 Computed tomography angiography images of a 54-year-old male who presented to the emergency department with acute chest pain that initially suggested aortic dissection. Coronary curve reconstructions showed proximal right coronary artery occlusion (arrow, *C*). Both radiologists and the deep-learning model assigned the right coronary artery to Class 3 and the left anterior descending artery (*A*) and circumflex artery (*B*) to Class 1. The probability histogram for classification of the right coronary artery by the deep-learning model is shown (*D*). Subsequent invasive coronary angiography confirmed the right coronary artery occlusion (arrow head, *E*), which was successfully recanalized by angioplasty (*F*).

technique did not show any major diagnostic benefit, being accompanied by a higher rate of non-contributory examinations and higher X-ray exposure.[28] Angiographic imaging of the aorta or coronary vessels remains conditional to accurate clinical and/or biological sorting upstream.

Our study had several limitations. The retrospective single-centre design and the exclusion of patients with histories of coronary interventions could have resulted in selection bias. Second, vessel centrelines were adjusted automatically by using dedicated software to limit human involvement and best approach real-life conditions. Whether manual centreline tracing would have optimized DLM performance was not evaluated. Third, the reference standard in our study was consensus image reading by two readers with differing levels of expertise, which could have weighed the result towards the more experienced reader. Finally, ICA was not performed routinely, and therefore, we could not assess the performance of the readers.

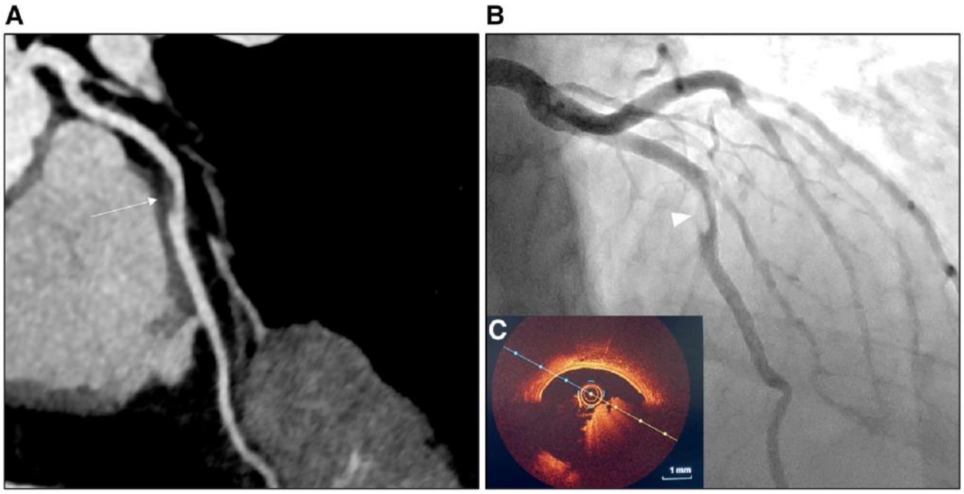

Figure 6 Computed tomography angiography images of a 39-year-old male who presented to the emergency department with persistent chest pain deemed atypical at clinical examination and modest troponin rise. An aortic computed tomography angiography was performed, with the coronary curve reconstruction (*A*) showing a soft plaque of the middle left anterior descending artery segment (arrow). Both human readers and deep-learning model rated the stenosis Class 2. Invasive coronary angiography (*B*) and optical coherence tomography (*C*) were performed the same day, showing a <50% stenosis (arrow head) due to a plaque with adjacent thrombotic material. A plaque rupture was diagnosed.

Conclusions

In this study, a DLM efficiently detected significant coronary stenosis in emergency room patients who underwent an ECG-gated aortic CTA to rule out aortic dissection. These findings highlight the potential value of AI models as diagnostic support for human analysis in an emergency setting.

Lead author biography

Dr Carl G. Glessgen is a board-certified radiologist currently working at the University Hospitals of Geneva. He completed his medical training at the University of Strasbourg and most of his residency at the University Hospital Basel, where he began focusing on clinical cardiac imaging. After two further years in Geneva, he now holds a position as attending radiologist in the cardiovascular imaging unit of Prof. Jean-Paul Vallée. His medical thesis was completed in 2019 on the topic of adverse gadolinium-based respiratory effects. Previous research collaborations include AI-based detection tools and optimization of diagnostic value for radiological images.

Data availability

The data underlying this article cannot be shared publicly because of individual privacy concerns. The data will be shared on reasonable request with the corresponding author.

Acknowledgements

The authors are grateful for the support of Anaëlle Steinert and Henri Giroussens for this work.

Funding

No funding was received for this study.

Conflict of interest: J.-F.P. is a founder and CEO of Spimed-AI. The other authors have no other disclosures to report.

References

1. Pittet V, Burnand B, Yersin B, Carron PN. Trends of pre-hospital emergency medical services activity over 10 years: a population-based registry analysis. *BMC Health Serv Res* 2014;**14**:380.
2. Owens PL, Barrett ML, Gibson TB, Andrews RM, Weinick RM, Mutter RL. Emergency department care in the United States: a profile of national data sources. *Ann Emerg Med* 2010;**56**:150–165.
3. Gulati M, Levy PD, Mukherjee D, Amsterdam E, Bhatt DL, Birtcher KK, Blankstein R, Boyd J, Bullock-Palmer RP, Conejo T, Diercks DB, Gentile F, Greenwood JP, Hess EP, Hollenberg SM, Jaber WA, Jneid H, Joglar JA, Morrow DA, O'Connor RE, Ross MA, Shaw LJ. 2021 AHA/ACC/ASE/CHEST/SAEM/SCCT/SCMR guideline for the evaluation and diagnosis of chest pain: executive summary: a report of the American College of Cardiology/American Heart Association Joint Committee on Clinical Practice Guidelines. *Circulation* 2021;**144**:e368–e454.
4. Erhardt L, Herlitz J, Bossaert L, Halinen M, Keltai M, Koster R, Marcassa C, Quinn T, van Weert H. Task force on the management of chest pain. *Eur Heart J* 2002;**23**:1153–1176.
5. Pacini D, Marco LD, Fortuna D, Belotti LMB, Gabbieri D, Zussa C, Pigini F, Contini A, Barattoni MC, De Palma R, Di Bartolomeo R. Acute aortic dissection: epidemiology and outcomes. *Int J Cardiol* 2013;**167**:2806–2812.
6. Hayter RG, Rhea JT, Small A, Tafazoli FS, Novelline RA. Suspected aortic dissection and other aortic disorders: multi-detector row CT in 373 cases in the emergency setting. *Radiology* 2006;**238**:841–852.
7. Kumamaru KK, Hoppel BE, Mather RT, Rybicki FJ. CT angiography: current technology and clinical use. *Radiol Clin North Am* 2010;**48**:213–235.
8. Isselbacher EM, Preventza O, Hamilton Black J, Augoustides JG, Beck AW, Bolen MA, Braverman AC, Bray BE, Brown-Zimmerman MM, Chen EP, Collins TJ, DeAnda A Jr, Fanola CL, Girardi LN, Hicks CW, Hui DS, Schuyler Jones W, Kalahasti V, Kim KM, Milewicz DM, Oderich GS, Ogbechie L, Promes SB, Gyang Ross E, Schermerhorn ML, Singleton Times S, Tseng EE, Wang GJ, Woo YJ. 2022 ACC/AHA guideline for the diagnosis and management of aortic disease: a report of the American Heart Association/American College of Cardiology Joint Committee on Clinical Practice Guidelines. *Circulation* 2022;**146**:e334–e482.
9. Ma GN, Hong H, Alwalid O, Cao YK, Hu XH, Han P, Gu J. Utility of ECG-gated CTA for detecting and classifying coronary artery involvement in patients with type A aortic

dissection and sinus of valsalva involvement. *AJR Am J Roentgenol* 2021;**217**: 1334–1343.

10. Hachulla AL, Ronot M, Noble S, Becker CD, Montet X, Vallée JP. ECG-triggered high-pitch CT for simultaneous assessment of the aorta and coronary arteries. *J Cardiovasc Comput Tomogr* 2016;**10**:407–413.
11. Schmuelling L, Franzeck FC, Nickel CH, Mansella G, Bingisser R, Schmidt N, Stieltjes B, Bremerich J, Sauter AW, Weikert T, Sommer G. Deep learning-based automated detection of pulmonary embolism on CT pulmonary angiograms: no significant effects on report communication times and patient turnaround in the emergency department nine months after technical implementation. *Eur J Radiol* 2021;**141**:109816.
12. Seyam M, Weikert T, Sauter A, Brehm A, Psychogios MN, Blackham KA. Utilization of artificial intelligence-based intracranial hemorrhage detection on emergent noncontrast CT images in clinical workflow. *Radiol Artif Intell* 2022;**4**:e210168.
13. Liu CY, Tang CX, Zhang XL, Chen S, Xie Y, Zhang XY, Qiao HY, Zhou CS, Xu PP, Lu MJ, Li JH, Lu GM, Zhang LJ. Deep learning powered coronary CT angiography for detecting obstructive coronary artery disease: the effect of reader experience, calcification and image quality. *Eur J Radiol* 2021;**142**:109835.
14. Chen M, Wang X, Hao G, Cheng X, Ma C, Guo N, Hu S, Tao Q, Yao F, Hu C. Diagnostic performance of deep learning-based vascular extraction and stenosis detection technique for coronary artery disease. *Br J Radiol* 2020;**93**:20191028.
15. Muscogiuri G, Chiesa M, Trotta M, Gatti M, Palmisano V, Dell'Aversana S, Baessato F, Cavaliere A, Cicala G, Loffreno A, Rizzon G, Guglielmo M, Baggiano A, Fusini L, Saba L, Andreini D, Pepi M, Rabbat MG, Guaricci AI, De Cecco CN, Colombo G, Pontone G. Performance of a deep learning algorithm for the evaluation of CAD-RADS classification with CCTA. *Atherosclerosis* 2020;**294**:25–32.
16. Hong Y, Commandeur F, Cadet S, Goeller M, Doris MK, Chen X, Kwiecinski J, Berman DS, Slomka PJ, Chang HJ, Dey D. Deep learning-based stenosis quantification from coronary CT angiography. *Proc SPIE Int Soc Opt Eng* 2019;**10949**:109492I.
17. Han D, Liu J, Sun Z, Cui Y, He Y, Yang Z. Deep learning analysis in coronary computed tomographic angiography imaging for the assessment of patients with coronary artery stenosis. *Comput Methods Programs Biomed* 2020;**196**:105651.
18. Han X, Luo N, Xu L, Cao J, Guo N, He Y, Hong M, Jia X, Wang Z, Yang Z. Artificial intelligence stenosis diagnosis in coronary CTA: effect on the performance and consistency of readers with less cardiovascular experience. *BMC Med Imaging* 2022;**22**:28.
19. Lin A, Manral N, McElhinney P, Killekar A, Matsumoto H, Kwiecinski J, Pieszko K, Razipour A, Grodecki K, Park C, Otaki Y, Doris M, Kwan AC, Han D, Kuronuma K, Flores Tomasino G, Tzolos E, Shanbhag A, Goeller M, Marwan M, Gransar H, Tamarappoo BK, Cadet S, Achenbach S, Nicholls SJ, Wong DT, Berman DS, Dweck M, Newby DE, Williams MC, Slomka PJ, Dey D. Deep learning-enabled coronary CT angiography for plaque and stenosis quantification and cardiac risk prediction: an international multicentre study. *Lancet Digit Health* 2022;**4**:e256–e265.
20. Paul JF, Rohnean A, Giroussens H, Pressat-Laffouilhere T, Wong T. Evaluation of a deep learning model on coronary CT angiography for automatic stenosis detection. *Diagn Interv Imaging* 2022;**103**:316–323.
21. Yi Y, Xu C, Guo N, Sun J, Lu X, Yu S, Wang Y, Vembar M, Jin Z, Wang Y. Performance of an artificial intelligence-based application for the detection of plaque-based stenosis on monoenergetic coronary CT angiography: validation by invasive coronary angiography. *Acad Radiol* 2022;**29**:S49–S58.
22. Zreik M, van Hamersvelt RW, Wolterink JM, Leiner T, Viergever MA, Isgum I. A recurrent CNN for automatic detection and classification of coronary artery plaque and stenosis in coronary CT angiography. *IEEE Trans Med Imaging* 2019;**38**:1588–1598.
23. Goetti R, Baumüller S, Feuchtner G, Stolzmann P, Karlo C, Alkadhi H, Leschka S. High-pitch dual-source CT angiography of the thoracic and abdominal aorta: is simultaneous coronary artery assessment possible? *AJR Am J Roentgenol* 2010;**194**:938–944.
24. Nazerian P, Mueller C, Soeiro AM, Leidel BA, Salvadeo SAT, Giachino F, Vanni S, Grimm K, Oliveira MT Jr, Pivetta E, Lupia E, Grifoni S, Morello F; ADvISED Investigators. Diagnostic accuracy of the aortic dissection detection risk score plus D-dimer for acute aortic syndromes: the ADvISED prospective multicenter study. *Circulation* 2018;**137**: 250–258.
25. Hoffmann U, Truong QA, Schoenfeld DA, Chou ET, Woodard PK, Nagurney JT, Pope JH, Hauser TH, White CS, Weiner SG, Kalanjian S, Mullins ME, Mikati I, Peacock WF, Zakroysky P, Hayden D, Goehler A, Lee H, Gazelle GS, Wiviott SD, Fleg JL, Udelson JE; ROMICAT-II Investigators. Coronary CT angiography versus standard evaluation in acute chest pain. *N Engl J Med* 2012;**367**:299–308.
26. Dedic A, Ten Kate GJ, Neefjes LA, Rossi A, Dharampal A, Rood PPM, Galema TW, Schultz C, Ouhlous M, Moelker A, de Feyter PJ, Nieman K. Coronary CT angiography outperforms calcium imaging in the triage of acute coronary syndrome. *Int J Cardiol* 2013;**167**:1597–1602.
27. Litt HI, Gatsonis C, Snyder B, Singh H, Miller CD, Entrikin DW, Leaming JM, Gavin LJ, Pacella CB, Hollander JE. CT angiography for safe discharge of patients with possible acute coronary syndromes. *N Engl J Med* 2012;**366**:1393–1403.
28. Burris AC, Boura JA, Raff GL, Chinnaiyan KM. Triple rule out versus coronary CT angiography in patients with acute chest pain: results from the ACIC consortium. *JACC Cardiovasc Imaging* 2015;**8**:817–825.